X-ray evidence for the relationship between pyridyl side chain basicity and the *Z/E* preferences of 5-halogen substituted (pyridin-2-yl)aminomethane-1,1-diphosphonic acids; implications for metal ions coordination in solution

Ewa Matczak-Jon,[a*] Katarzyna Ślepokura,[b] and Barbara Kurzak[c]

[a]*Department of Chemistry, Wrocław University of Technology, Wybrzeże Wyspiańskiego 27, 50-370 Wrocław, Poland*
[b] *Faculty of Chemistry, University of Wrocław, Joliot-Curie 14, 50-383 Wrocław, Poland*
[c] *Faculty of Chemistry, University of Opole, Oleska 48, 45-052 Opole, Poland*
E-mail: ewa.matczak-jon@pwr.wroc.pl

Dedicated to Prof. Paweł Kafarski to honor the achievements within his career

DOI: http://dx.doi.org/10.3998/ark.5550190.0013.412

Abstract

The crystal structures of three salts (**1-a**–**3-a)**, products of the reactions between 5-chloro (**1**), 5-bromo (**2**) and 5-iodo (**3**) substituted (pyridin-2-yl)aminomethane-1,1-diphosphonic acids and 4-aminopyridine were determined by single crystal X-ray diffraction and discussed with respect to molecular geometry and solid state organization. In all **1-a**–**3-a**, bisphosphonate dianion adopts the opposite (*E*) conformation with respect to the C2–N1 bond, compared with the parent zwitterion. This provides further evidence that intermolecular N–H···O hydrogen bonds involving both exocyclic and pyridinium N atoms as proton donors and an O atom of the phosphonic/phosphonate group as acceptor play a significant role in stabilizing the *Z* conformation of this particular subclass of acids. The solution behavior and complex-formation abilities of [(5-iodopyridin-2-yl)amino]methane-1,1-diphosphonic acid (**3**) were also studied. Compound **3** exists in solution as the *Z*/*E* mixture. However, the barrier to rotation around the C2–N1 bond in **3** is lower, compared with **1** and **2**. This is important for the complex-formation processes in the Zn(II), Mg(II) and Ca(II) solutions with **3**.

Keywords: Bisphosphonates, X-ray structures, complex-formation equilibria, NMR, potentiometry, ESI-MS

Introduction

Bisphosphonates are widely used to treat bone resorption diseases such as osteoporosis, Paget 's disease and osteolytic bone metastases.[1] The most potent of them with at least one nitrogen atom in their side chain, NBP's, act by inhibiting the farnesyl pyrophosphate synthase (FPPS), a key regulatory enzyme in the mevalonate pathway common in human, parasitic protozoa and plant cells.[2]

A prominent group among NBP's are (pyridinyl)aminomethane-1,1-diphosphonic acids with a direct C_{α}–N_{amino} bond. Although the first reported synthesis and biological activity of this subclass of acids dates back to 1979,[3] these compounds attracted marginal attention until it has been demonstrated that they kill bacteria and pathogenic protozoa such as *Plasmodium or Trypanosoma* parasites,[4] and inhibit the FPPS at micro- or even nanomolar level.[5] In a series of our previously published papers we have demonstrated that (pyridin-2-yl)aminomethane-1,1-diphosphonic acids can occur as the two (*Z* or *E*) conformers with respect to partial double C2–N1 bond (mean length *c.a*. 1.35 Å) with the C1–N1–C2–C3 torsion angle being close to 0 or 180°, respectively (scheme 1a).

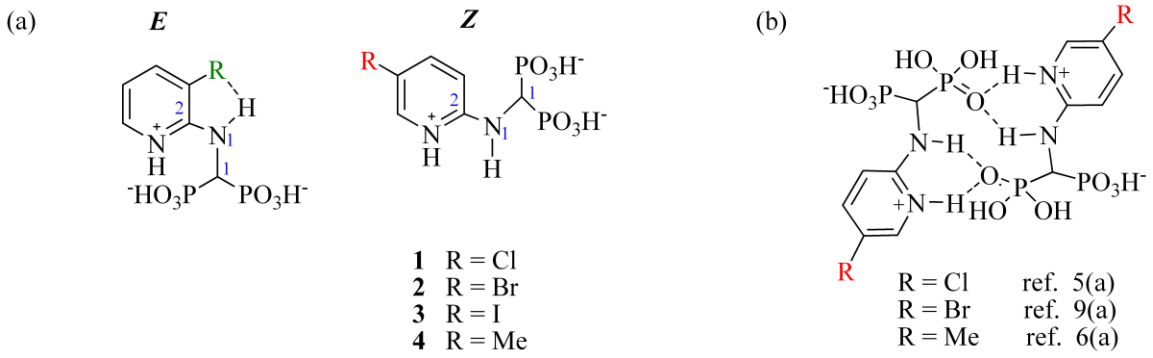

Scheme 1. (a) *Z* and *E* assignments according to ref. 6(a), (b) N–H···O hydrogen bonded dimer common for the *Z*-zwitterions of **1**, **2** and **4**.

Interestingly, compounds with a substituent attached at 3-ring position prefer the *E* conformation in both the solid state and in solution[6] even in the presence of other substituents attached to the pyridine ring.[7] A key role in the stabilization of the *E* conformer plays the intramolecular N–H···X hydrogen bond involving the exocyclic N atom as a proton donor and the sterically accessible substituent as a proton acceptor (Scheme 1a). On the other hand, compounds with a substituent at 4- or 5- ring position and unsubstituted C3 atom exist in solution as the Z/E mixture[6(a),8] while their zwitterions crystallize as the *Z* conformers.[5(a),6(a),9(a)] A common feature of the *Z*-zwitterions is that their conformation is stabilized through intermolecular N–H···O interactions involving protonated N_{py} and N1 atoms (Scheme 1b).

The crystal structures of the salts comprising 5-methyl-substituted (pyridin-2-yl)aminomethane-1,1-diphosphonate anion and 4-aminopyridinium or ammonium cations, respectively, have revealed that the removal of the proton from the pyridinium N atom relaxes the strain imposed on the *Z* conformer by N–H···O hydrogen bonds, and as a result the *E* form is able to crystallize from a solution.[9(b)] A supporting evidence for this observation has been provided by the crystal structure of the disodium salt of **1**, which reveals that the [(5-chloropyridin-2-yl)amino]methane-1,1-diphosphonate dianion also adopts the *E* conformation.[5(a)] In order to corroborate the generality of these relations the crystal structures of three salts **1-a**, **2-a** and **3-a** have been determined. The asymmetric unit of each **1-a**–**3-a** comprises 5-halogen (Cl, Br, I) substituted (pyridin-2-yl)aminomethane-1,1-diphosphonate dianion $(LH_2)^{2-}$, two 4-aminopyridinium cations and four water molecules (Scheme 2).

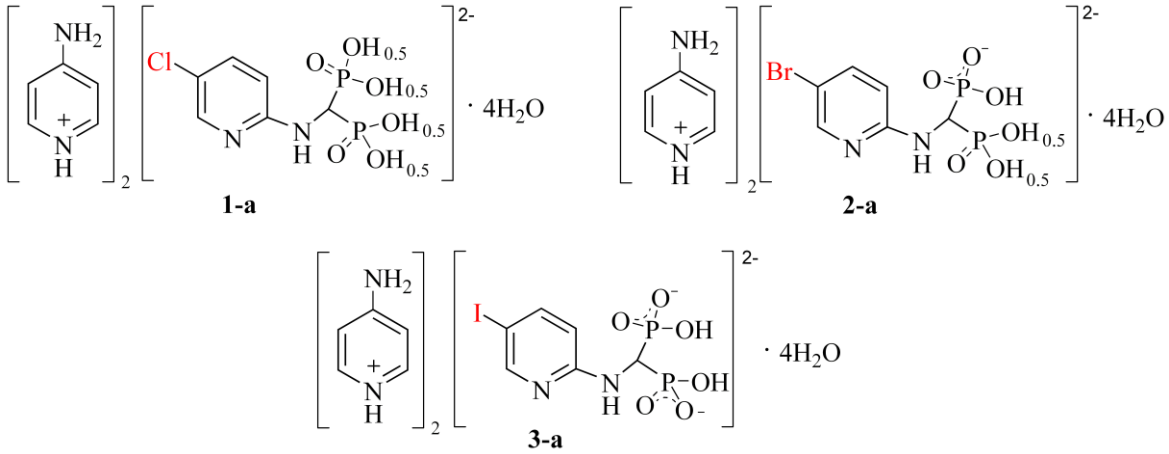

Scheme 2. Graphical representation of **1-a**, **2-a** and **3-a**.

Notable is that the pK_a values attributed to a proton dissociation from the N_{py} atom of **1**, **2** and **3** are markedly lower compared to **4** and this correlates well with the rotational barrier around the C2–N1 bond, $\mathbf{3}^{\text{this work}} < \mathbf{1}^{10} \sim \mathbf{2}^{10} < \mathbf{4}$.[8(a)] Recently, we have demonstrated that a decrease in the rotational barrier of **1** and **2**, compared with **4**[8(a)] significantly affects complex-formation processes in their solutions.[10] In the case of **4**, which has exceptionally basic pyridyl nitrogen atom (pK_{NH^+} = 8.18), N–H···O intermolecular interactions stabilize the *Z* ligand conformation over a broad range of pH. For **1** and **2**, the range of pH in which the *Z* conformer is stabilized by similar intermolecular interactions is significantly narrower. As a result, the *Z* ligand conformation is preferred in multinuclear Zn(II), Mg(II) and Ca(II) complexes of **4** over a broad range of pH, while the loss of conformational stabilization is likely the reason that complexation processes taking place in the M(II) solutions with **1** and **2** are complicated by the intramolecular *Z*/*E* interconversion. In order to gain a better understanding of this phenomenon herein we present similar studies on the Zn(II), Mg(II) and Ca(II) complexation by **3**.

Results and Discussion

Crystal structures and intermolecular interactions in 1-a, 2-a and 3-a

The crystals of **1-a**, **2-a** and **3-a** are isomorphous, with the overall molecular structures of the anions and the crystal packing schemes being very similar. The asymmetric unit and atom-numbering scheme for the representative salt **3-a** are shown in Fig. 1. Selected geometrical parameters for all **1-a**–**3-a** are listed in Table 1. In **3-a**, one proton is located on atom O3 and the other on atom O6, respectively. In contrast, some of the bisphosphonate H atoms in **1-a** and **2-a** are disordered over two sites and were refined with s.o.f. = 0.5 each, at two different O atoms (see Experimental Part).

In agreement with the crystal structures of **1**[5(a)], **2**[9(a)] and related bisphosphonic acids,[6–8(a),10] atom N1 of each dianion in **1-a–3-a** is sp^2-hybridized. This results in partial-double bond character of the N1–C2 bond (1.356(3) Å, 1.364(3) Å and 1.366(2) Å for **1-a, 2-a** and **3-a**, respectively) and near-coplanarity of the N1 and C1 atoms with the pyridine ring. Each dianion adopts the *E* conformation, which is in contrast to the Z-zwitterions of **1** and **2**. This is reflected in the values of the C1–N1–C2–C3 torsion angle of -179.7(2)°, 179.6(2)°, and 179.4(2)° for **1-a**, **2-a** and **3-a**, respectively, and of 6.52°, 13.36° for **1** (two zwitterions in the asymmetric unit)[5(a)] and 0.5(4)° for **2**.[9(a)]

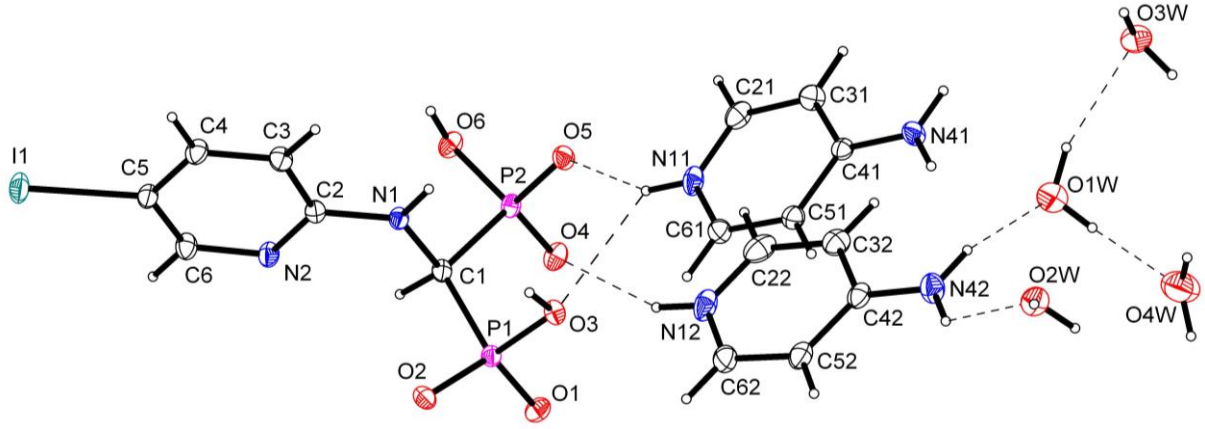

Figure 1. The molecular structure of the representative salt **3-a**, with the atom-numbering scheme and hydrogen bonds shown with dashed lines (disorder of water molecules omitted for clarity). Displacement ellipsoids are shown at the 50% probability level.

A common phenomenon in the crystal structures of most of (pyridinyl)aminomethane-1,1-diphosphonic acids examined to date is an almost planar *W* conformation of the (H)O–P1–C1–P2–O sequence, which enables the formation of the $(P–C–P–O–H\cdots O)_n$ chains.[5(a),6(a),7,8(a),9]. In the dianions of **1-a** and **2-a**, the *W* conformation of the O–P1–C1–P2–O sequence involves atoms O2 and O5. In **3-a**, atoms O2 and O6 are involved. This is reflected in the O2–P1–C1–P2 and O5/O6–P2–C1–P1 torsion angles of -177.21(11)°, -178.99(11)° for **1-a**, -176.46(12)°, -178.11(11)° for **2-a**, and 175.80(9)°, 174.42(9)° for **3-a**, and results in the

formation of an uncommon type of chains (Fig. 2a). The overall architecture of the chains is similar. In **1-a** and **2-a** (with disordered bisphosphonate H atoms), the chains are generated through the O2···O3 and O5···O6 contacts between the adjacent dianions. In **3-a** (with the phosphonate H atoms located at O3 and O6), these are the O3–H3···O2^{i} and O6–H6···O5^{ii} interactions. Indeed, in **3-a**, an additional stabilization is provided by the N1–H1*N*···O2^{i} contact (Fig 2a, Table S1).

In all **1-a–3-a**, the chains are held together into crystal lattice by hydrogen bonds involving aminopyridinium cations and water molecules (Fig 2b, Table S1).

Table 1. Selected interatomic distances (Å), bond angles (deg) and torsion angles (deg) for **1-a, 2-a** and **3-a**

	1-a	**2-a**	**3-a**
Bond lengths			
P1–O1	1.491(2)	1.488(2)	1.499(2)
P1–O2	1.524(2)	1.539(2)	1.520(2)
P1–O3	1.552(2)	1.557(2)	1.585(2)
P2–O4	1.491(2)	1.492(2)	1.498(2)
P2–O5	1.532(2)	1.525(2)	1.518(2)
P2–O6	1.557(2)	1.573(2)	1.584(2)
P1–C1	1.821(2)	1.818(2)	1.830(2)
P2–C1	1.816(3)	1.815(2)	1.828(2)
N1–C1	1.455(2)	1.459(3)	1.461(2)
N1–C2	1.356(3)	1.364(3)	1.366(2)
C5–halogen	1.729(3)	1.891(3)	2.095(2)
Bond angles			
O1–P1–O2	113.78(11)	112.63(10)	116.49(9)
O1–P1–O3	110.74(10	111.66(10)	108.77(9)
O2–P1–O3	110.18(10)	109.77(10)	109.34(8)
O1–P1–C1	110.85(10)	111.09(10)	110.77(8)
O2–P1–C1	105.83(10)	105.92(11)	106.71(9)
O3–P1–C1	105.00(10)	105.37(10)	104.03(8)
O4–P2–O5	114.83(10)	116.01(10)	116.74(9)
O4–P2–O6	110.99(11)	110.22(10)	108.89(8)
O5–P2–O6	108.91(10)	108.91(9)	109.43(8)
O4–P2–C1	110.94(11)	110.53(10)	110.06(9)
O5–P2–C1	105.87(11)	106.22(10)	107.27(8)
O6–P2–C1	104.69(11)	104.24(10)	103.64(9)
P1–C1–P2	116.7(2)	117.0(2)	115.3(1)

Table 1. (Continued)

P1–C1–N1	108.1(2)	108.1(2)	109.5(2)
P2–C1–N1	109.1(2)	108.8(2)	108.0(2)
C1–N1–C2	126.1(2)	126.7(2)	124.7(2)
Torsion angles			
C2–N1–C1–P1	-114.0(2)	-114.7(2)	-110.8(2)
C2–N1–C1–P2	118.2(2)	117.4(2)	122.9(2)
C1–N1–C2–N2	0.4(3)	-0.4(3)	-1.2(3)
C1–N1–C2–C3	-179.7(2)	179.6(2)	179.4(2)

(a)

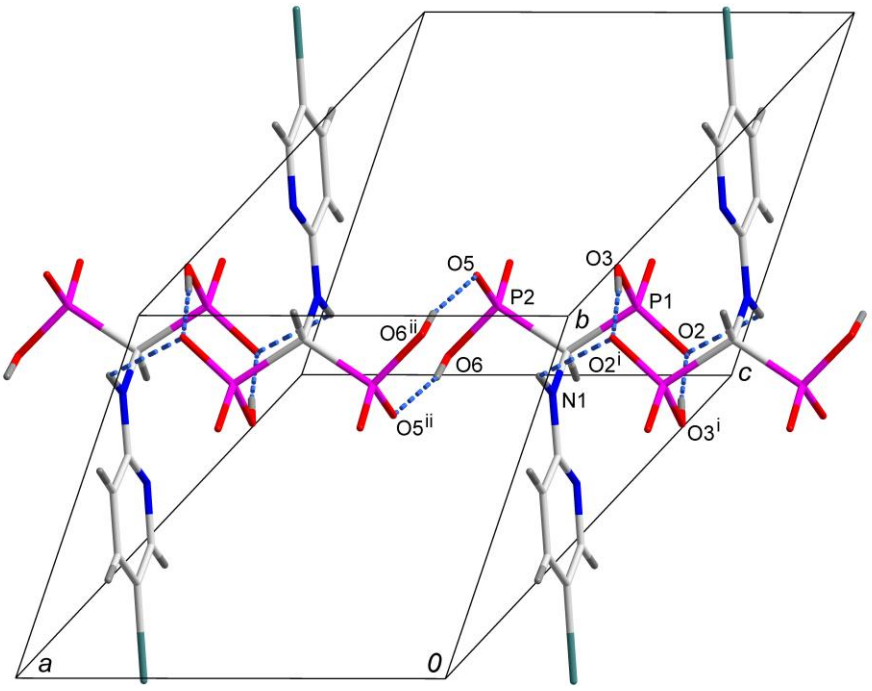

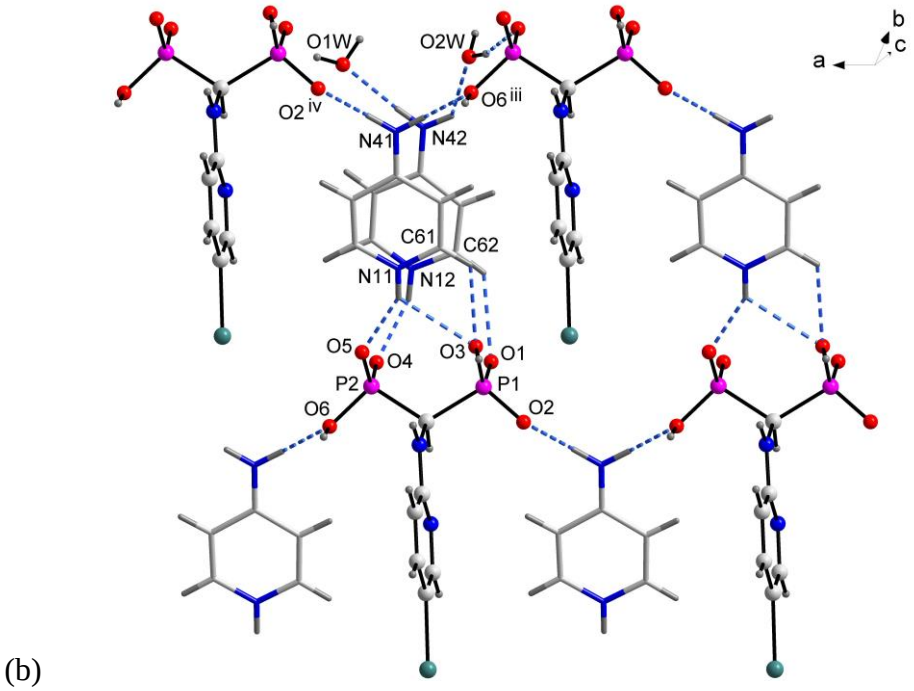

(b)

Figure 2. Intermolecular interactions in the crystal lattice of **3-a**. (*a*) The dianions joined through the O3–H3···O2^{i}, O6–H6···O5^{ii} and N1–H1*N*···O2^{i} contacts (dashed lines) to form chains along *a*-axis. (*b*) Interactions between bisphosphonate anions, aminopyridinium cations and water molecules. Symmetry codes are given in Table S1.

Solution properties of 3

Compound **3** contains five dissociable protons in the fully protonated form, $[H_5L]^+$. The p*Ka* values corresponding to the first proton dissociation from the PO_3H_2 groups lie in the range ~1.5–2, therefore, only three dissociation processes could be detected under experimental conditions. The pK_a value of 4.69 corresponds to the proton dissociation from the N_{py} atom. The next proton dissociation takes place on more acidic PO_3H^- group (pK_a = 6.73). The release of the proton from more basic PO_3H^- group yields the pK_a value of 9.95. All p*Ka* values compare well with those determined previously for **1** and **2.**[10] Indeed, the protonation schemes in the crystals of **1**[5(a)], **2**[9(a)], related dianions of **1-a**–**3-a** (scheme 2) and disodium salt of **1**[5(a)] reveal that the sequence of protons dissociation in **3**, NH_{py}^+, PO_3H^-, PO_3H^-, is the same as in **1** and **2**.

The dynamic NMR experiment has indicated that the temperature-dependence of the ^{31}P NMR spectra of **3** is similar to that reported for **1** and **2**.[10] The spectra recorded under analogous experimental conditions (see experimental part) reveal substantial line broadening upon gradual decrease in a temperature. This indicates that similar to 5-Cl and 5-Br-substituted analogs, compound **3** exists in solution as a mixture of the *Z* and *E* conformers. However, unlike **1** and **2**, which spectra demonstrate splitting of the ^{31}P NMR resonance in the temperature range 243-238 K (Fig 3a), the only observed effect of a temperature on the ^{31}P NMR spectra of **3** is increase in line width upon sample cooling, even at 228 K, which is the lowest achievable temperature (Fig

3b). This clearly indicates, that the barrier to rotation around the C2–N1 bond in **3** is lower compared to **1** and **2** ($\Delta G^{\#}$ = 47.6 kJ/mol^{-1} and 47.8 kJ/mol^{-1}, respectively),[10] and cannot be determined experimentally by the NMR method.

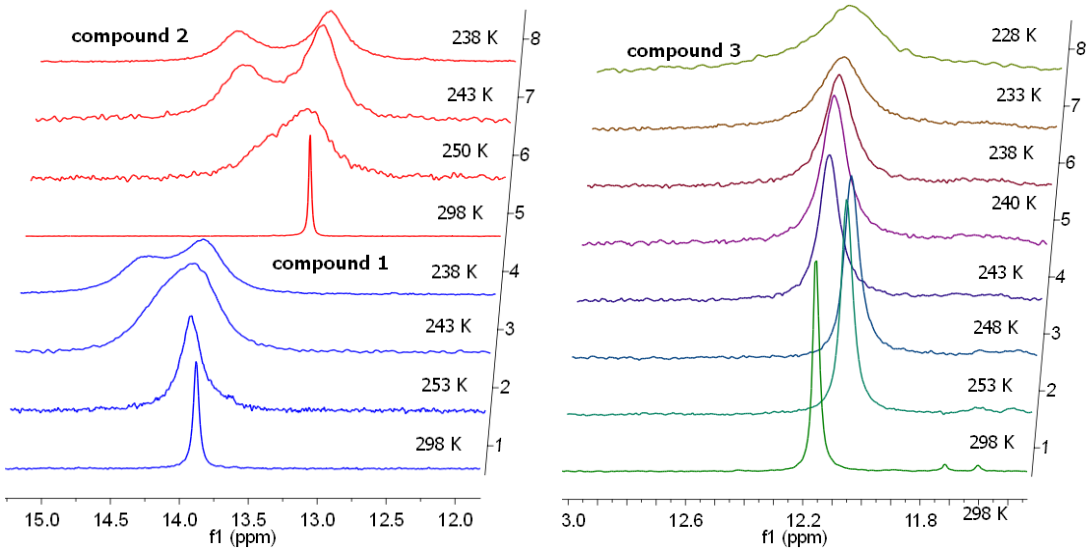

Figure 3. Dynamic ^{31}P NMR spectra of **1**, **2** (left) and **3** (right) over a temperature range 238(228) - 298 K (for details see also ref. 10).

Zn(II), Mg(II) and Ca(II) complexes with 3

Recently we have demonstrated that the formation of soluble, protonated multinuclear complexes in the Zn(II), Mg(II) and Ca(II) solutions with (pyridin-2-yl)aminomethane-1,1-diphosphonic acid and related 4- and 5-substituted derivatives is exceptionally slow on the NMR time-scale, compared with most of bisphosphonates. Indeed, the complex-formation processes are dependent on the rotational barrier around the C2–N1 bond.[10] Compound **3** exhibits similar spectral behavior. In particular, the ^{31}P NMR spectra of the equimolar Zn(II)–**3** system recorded at pH *ca.* 7–9 reveal disordered, non-resolvable set of signals with chemical shifts and spectral pattern similar to those observed for analogous systems with **1** and **2** (Figure 4, left), however, significantly different from those observed for **4**.[10]. Accordingly, a set of resonances corresponding to the C1H1 proton and broad, difficult to resolve signals attributed to protons H3, H4 and H6 have been detected in the corresponding ^{1}H NMR spectra. This indicates that the range of pH in which the *Z* conformation of **3** is stabilized in solution through intermolecular hydrogen bonds is similar to that observed for **1** and **2**, and is significantly narrower compared to **4**. Thus, similar to the spectra of the Zn(II) equimolar systems with **1** and **2**, both ^{31}P and ^{1}H NMR spectra of the related Zn(II) system with **3** reflect two overlapped difficult to distinguish processes: slow (on the NMR time scale) metal-ligand exchange corresponding to the formation of multinuclear complexes and slow Z/E interconversion of the metal-coordinated ligands.

On the other hand, under ligand excess relative to Zn(II), the ^{31}P NMR spectra of all **1**–**4** display a single resonance (Figure. 4, right), which is moved downfield in relation to metal-free ligand. This strongly suggests that under these conditions simple mononuclear Zn(II) complexes may be expected in solution.

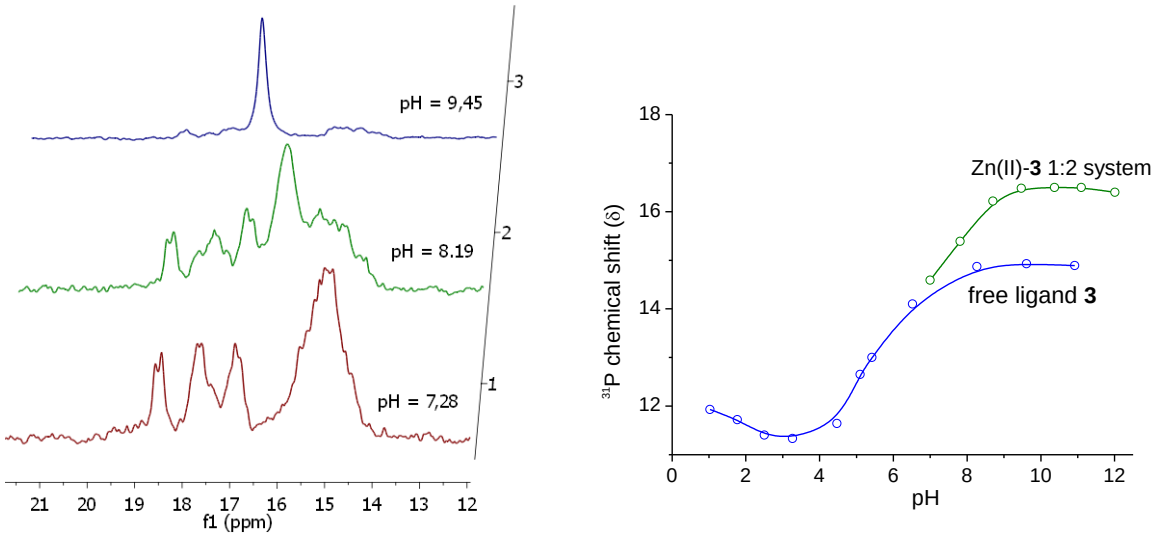

Figure 4. Representative ^{31}P NMR spectra for the Zn(II) equimolar systems with **3** (left). ^{31}P titration curves *versus* pH for the Zn(II)–**3** 1:2 molar system and for metal-free ligand **3** (right).

A distinguished feature of **3** compared to **1** and **2**[10] is, however, stronger tendency for the formation of insoluble Mg(II) and Ca(II) complexes at metal and ligand concentrations used in NMR studies. Similar behavior has been observed for analogous systems with bisphosphonates containing 1,3(thiazol-2-yl) and 1,3(benzothiazol-2-yl) side chains. Taking into consideration that intramolecular dynamics of both these compounds is similar to that observed for **3**,[10] one can presume that an important reason for such behavior may be a decrease in rotational barrier for the Z/E interconversion compared to **1** and **2**.

In order to establish stoichiometries of the complexes formed in the Zn(II), Mg(II) and Ca(II) solutions with **3**, the ESI-MS experiments have been performed. This technique is not able to define the number of ionizable protons in the species. However, the determination of their molecular weight, charge, and isotopic distribution patterns offers a powerful tool for the elucidation of stoichiometries of metal complexes preformed in solution. Indeed, series of adducts with the same M(II):ligand ratio and variable number of alkali cations seem to be a good indication of reliability of stoichiometric recognition.[10-13]

The assignments of the most prominent peaks in the positive and negative ion mode ESI-MS spectra for the Zn(II), Mg(II) and Ca(II) complexes with **3** are summarized in Table 2. The experimental and calculated isotope distribution patterns for the representative Zn(II) complexes are given in Figure 5.

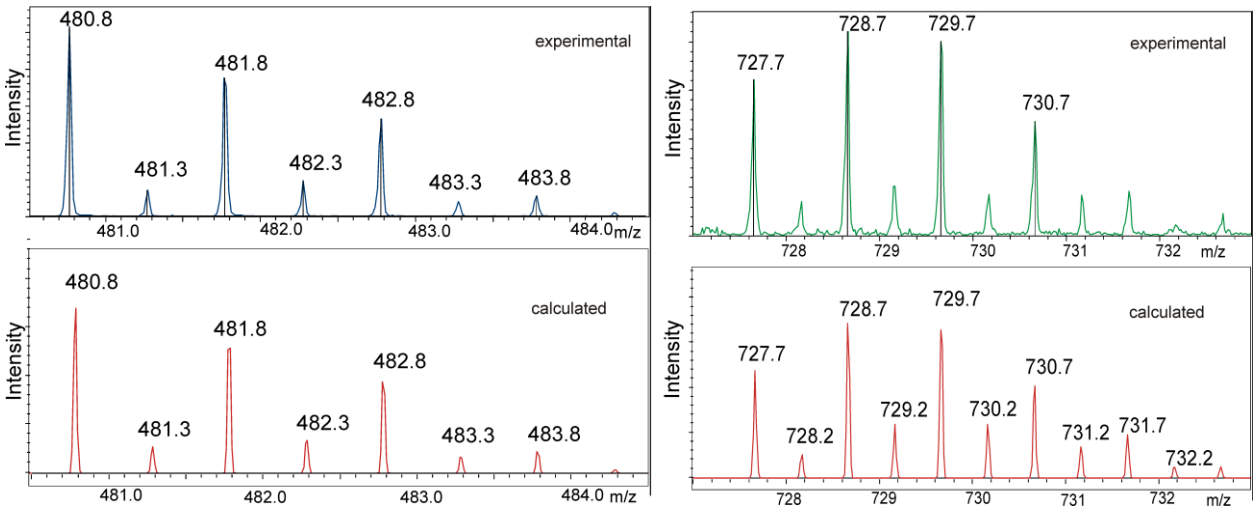

Figure 5. Experimental and calculated isotope distribution patterns for the representative $[Zn(HL_2)K_3]^{2-}$ (left) and $[Zn_2(H_2L_3)K_4]^{2-}$ (right) complexes with **3**.

In general, 1:2 and 2:3 M(II):ligand molar ratio species, predominantly adducts with different number of K^+ or Na^+ ions, have been found as the most abundant. These species are detected as double charged ions in the spectra acquired in both positive and negative-ion mode. In addition, the ESI-MS spectra have revealed peaks corresponding to the metal free ligand adducts with K^+ or Na^+(mostly singly charged), and higher mass 2:4 metal-to-ligand ratio complexes. The latter species are likely gas condensation products of lower mass 1:2 M(II):ligand molar ratio ions.

In view of the above consideration, the pH-potentiometric calculations were performed for the Zn(II), Mg(II) and Ca(II) systems with **3**. The stability constants of the complexes were calculated based on the assumption that stoichiometries of the most chemically significant complexes are consistent with stoichiometries detected by the ESI-MS method. The best fits between the experimental and calculated pH-metric titration curves have been obtained by assuming the species given in Table 3.

According to these data, all the systems have the same equilibrium model, in which dinuclear $[M_2L_3H_x]$ (x = 3, 4, 6) complexes are formed in a broad pH range while mononuclear $[ML_2H]$ and hydroxo [MLOH] complexes are predominant in basic solutions.

As seen in Figure 6, dinuclear$[Zn_2L_3H_6]$ species is formed at very low pH while the related Mg(II) and Ca(II) complexes are detected above pH=3. A gradual loss of protons with the increase in pH leads to the $[M_2L_3H_4]$ and $[M_2L_3H_3]$ complexes. In all three systems the $[M_2L_3H_3]$ species are detected at close to neutral pH and according to the NMR experiments have higher solubility in water, compared with those having higher number of protons. Under ligand excess, the $[ZnL_2H]$ complex dominates in the pH range *c.a.* 7–9, whereas corresponding Mg(II) and Ca(II) complexes are detected in the pH range *c.a.* 7.5–9 and 8–9, respectively. The logβ values determined for these species decrease in the order: 25.55> 19.99 > 18.80, thus,

indicating that the $[ZnL_2H]$ complex is the most stable, while the stability of the related Ca(II) complex is only *c.a.* one order of magnitude lower than that of the $[MgL_2H]$ complex. A comparison of the stabilities of the $[MgL_2H]$ and $[CaL_2H]$ complexes of **3** and **2**[10] reveals that in spite of similar basicities of the coordinating donor groups, complexes of **3** are about 1.4 order of magnitude more stable than those of **2**.

Compound **3** forms with the Zn(II), Mg(II) and Ca(II) ions exclusively O-bonded complexes, in which the M(II) ions are coordinated through oxygen atoms of the phosphonate groups. This is reflected in chemical shift values of the ^{31}P NMR resonances (Fig. 4), which compare well with those determined for analogous systems with **1** and **2**.[10]

Table 2. Major peks identified in the ESI-MS spectra of the 1:2 and 1:1 molar ratio systems of Zn((II), Mg(II) and Ca(II) with **3** and the corresponding species found by potentiometry

	Negative ion mode		Positive ion mode		Corresponding
M(II):L system	Peaks *m/z*	Stoichiometries	Peaks *m/z*	Stoichiometries	species found by potentiometry
Zn(II)–**3**	461.8	$[Zn(H_2L_2)K_2]^{2-}$	577.7	$[Zn(L)_2K_6]^{2+}$	
	480.8	$[Zn(HL_2)K_3]^{2-}$			$[ZnL_2H]$
	499.8	$[Zn(L_2)K_4]^{2-}$			
	708.7	$[Zn_2(H_3L_3)K_3]^{2-}$	824.6	$[Zn_2(HL_3)K_9]^{2+}$	
	727.6	$[Zn_2(H_2L_3)K_4]^{2-}$	843.5	$[Zn_2(L)_3K_{10}]^{2+}$	
	746.6	$[Zn_2(HL_3)K_5]^{2-}$			$[Zn_2L_3H_6]$
	765.6	$[Zn_2(L_3)K_6]^{2-}$			$[Zn_2L_3H_4]$
	962.6	$[Zn(HL)_2K_3]^{-}$			$[Zn_2L_3H_3]$
	924.6	$[Zn(H_3L_2)K_2]^{-}$			
			964.6	$[Zn_2(H_2L)_4K_6]^{2+}$	
Mg(II)–**3**	414.9	$[Mg(HL)]^{-}$	530.7	$[Mg(L)K_3]^{+}$	$[MgLH_{-1}]$
	460.9	$[Mg(HL_2)K_3]^{2}$	784.6		$[MgL_2H]$
	479.8	$[Mg(L_2)K_4]^{2}$	803.6		
	668.7	$[Mg_2(H_3L_3)K_3]^{2-}$		$[Mg_2(HL_3)K_9]^{2+}$	$[Mg_2L_3H_6]$
	687.8	$[Mg_2(H_2L_3)K_4]^{2-}$		$[Mg_2(L_3)K_{10}]^{2+}$	$[Mg_2L_3H_4]$
	706.8	$[Mg_2(HL_3)K_5]^{2-}$			$[Mg_2L_3H_3]$
	725.8	$[Mg_2(L_3)K_6]^{2-}$			
			1076.4	$[Mg_2(L_4)K_{14}]^{2+}$	
Ca–**3**	430.9	$[Ca(HL)]^{-}$	498.8	$[Ca(L)Na_3]^{+}$	$[CaLH_{-1}]$
	452.8	$[Ca(L)Na]^{-}$			
	422.9	$[Ca(H_3L_2)Na]^{2-}$			$[Ca_2L_3H_6]$
	660.8	$[Ca_2(H_3L_3)Na_3]^{2-}$			$[Ca_2L_3H_4]$
	671.8	$[Ca_2(H_2L_3)Na_4]^{2-}$			$[Ca_2L_3H_3]$
			958.6	$[Ca_2(H_2L_4)Na_{12}]^{2+}$	

Table 3. Stability constants ($\log\beta_{pqr}$ values), for the proton, Zn(II), Mg(II) and Ca(II) complexes with **3**, T=298 K, I = 0.2 mol·dm^{-3} (KCl)

Species*	p q r			
Ligand **3**	0 1 1		9.95(4)	
	0 1 1		16.68(7)	
	0 1 3		21.37(8)	
pK_1			9.95	
pK_2			6.73	
pK_3			4.69	
M(II):**3** systems		Zn(II)	Mg(II)	Ca(II)
$[M_2L_3H_6]$	2 3 6	68.25(9)	63.53(7)	63.48(10)
$[M_2L_3H_4]$	2 3 4	60.30(10)	51.42(8)	51.14(12)
$[M_2L_3H_3]$	2 3 3	54.55(17)	44.22(11)	43.74(17)
$[ML_2H]$	1 2 1	25.55(9)	19.99(5)	18.80(7)
$[MLH_{-1}]$	1 1 -1	2.06(12)	-3.91(6)	-4.58(7)
χ^2		11.26	4.74	2.06
σ		7.96	8.41	11.98

*The constants are calculated for the equilibrium: $pM + qL + rH = M_pL_qH_r$

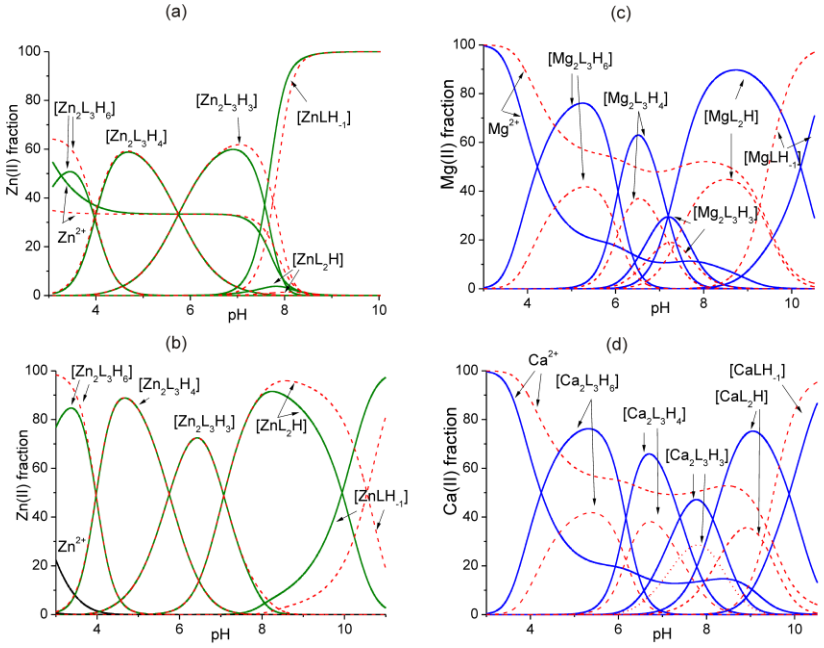

Figure 6. Species distribution diagrams for the Zn(II), Mg(II) and Ca(II) systems with **3** as a function of pH. (a) Zn(II)–**3** system at 1:1 molar ratio; (b) Zn(II)–**3** system at 1:2 molar ratio

[solid line - c_M = 1 x 10^{-3} mol dcm^{-3} (potentiometric conditions) dashed line - c_M = 1 x 10^{-2} mol dcm^{-3} (simulated for NMR conditions)]; (c) Mg(II)–**3** system, c_M = 1 x 10^{-3} mol dcm^{-3}, 1:1 molar ratio (solid line) and 1:2 molar ratio (dashed line); (d) Ca(II)–**3** system, c_M = 1 x 10^{-3} mol dcm^{-3}, 1:1 molar ratio (solid line) and 1:2 molar ratio (dashed line).

It is to note, that the binding affinity of **3** for Mg(II) and Ca(II) is similar to that calculated for **1** and **2**.[10] This is reflected in the pM values of 3.31 and 3.32, respectively; p[M] – the negative logarithm of the free metal ion concentration calculated under identical conditions (pH =7.0, 1:1 metal-to-ligand molar ratio, $c_M = 1 \cdot 10^{-3}$ M). The related pM value calculated for the Zn(II)–**3** system is equal 3.47.

Conclusions

The crystal structures of **1-a**–**3-a** have been determined, which demonstrate that a loss of conformational stabilization provided by intermolecular N–H···O hydrogen bonds upon proton release from the pyridinium N atom leads to opposite conformation of the dianions of **1, 2** and **3**, compared with the parent zwitterions. This indirectly confirms that as long as the pyridinium N atom remains protonated these intermolecular interactions play a crucial role in stabilizing the *Z* conformation of this particular subclass of bisphosphonates in both the solid state and in solution.

The combined NMR, potentiometric and ESI-MS studied have provided information on the solution behavior and complex-formation abilities of **3**. Compound **3** exists in solution as the *Z*/*E* mixture, which is similar to that observed for **1** and **2**. However, the barrier to rotation around the C2–N1 bond is lower in **3** compared with its 5-Cl and 5-Br substituted analogs.

Similar to previously studied **1**, **2** and **4**, compound **3** shows strong tendency for the formation of protonated multinuclear complexes at 1:1 metal-to-ligand molar ratio, and this process is slow on the NMR-time scale in solution. Similar to **1** and **2** and in contrast to **4**, the most likely reason for spectral behavior reflected in the NMR spectra of the Zn(II), Mg(II) and Ca(II) solutions with **3** is the loss of conformational stabilization for the *Z* conformer at relatively low pH, which results in two overlapped, difficult to distinguish processes: slow on the NMR time-scale metal-ligand exchange and slow Z/E interconversion of metal-coordinated ligands.

All the M(II) (M = Zn, Mg, Ca) systems with **3** have the same equilibrium model, in which dinuclear [$M_2L_3H_x$] (x = 3, 4, 6) complexes are formed in a broad pH range, while mononuclear [ML_2H] and hydroxo [MLOH] complexes are predominant in basic solutions. Notable is that **3** exhibits similar affinity for Mg(II) and Ca(II), and that stabilities of the related Ca(II) and Mg(II) complexes differ form each other by only *ca.* 0.5 - 1 order of magnitude.

Experimental Section

Materials. Compounds **1**–**3** were obtained according to the previously described procedures.[14] For details for **1** and **2** see Refs. 5(a), 9(a) and 10. NMR characteristics of **3**: (D_2O, pH = 7.04) ^{1}H NMR (ppm, ref. TMS): δH1 4.00 (1H, t, ^{3}JPH = 19.3 Hz), δH3 6.49 (1H, d, ^{3}JHH = 8.8 Hz), δH4 7.64 (1H, dd, ^{3}JHH = 8.8 Hz, ^{4}JHH = 2.3 Hz), δH6 7.98 (1H, d, ^{4}JHH = 2.3 Hz); ^{13}C NMR (ppm, ref. TMS): δC1 50.3 (^{1}JPC = 124.2 Hz), δC2 156.6 (^{3}JPC = 3.1 Hz), δC3 111.3, δC4 146.1, δC5 74.6, δC6 150.9; ^{31}P NMR (ppm, ref. 85% H_3PO_4) δP 14.6.

The metal(II) stock solutions for potentiometric measurements were prepared from MCl_2 Titrisol (Merck) concentrates. The exact metal ion concentration was checked by complexometric ethylenediaminetetraacetate (EDTA) titration. Carbonate-free potassium hydroxide solution (the titrant) was prepared from KOH and standardized against a standard potassium hydrogen phthalate solution. HCl solution was purchased from Merck as a Titrisol concentrate for preparation of stock solutions. The exact concentrations of Titrisol stock solutions and the ligand stock solutions were determined by the Gran's method.[15] All solutions were prepared with the use of bi-distilled water.
Nitrate salts of Zn(II), Mg(II) and Ca(II) (Aldrich) were used as a source of the metal ions in the NMR and ESI-MS studies. All chemicals and solvents were used without further purification.

Crystals preparation. General procedure to obtain salts **1-a, 2-a** and **3-a**: 0.050 g (0.16 mmol of **1,** 0.14 mmol of **2** or 0.13 mmol of **3**) and 0.32 mmol, 0.28 mmol or 0.26 mmol of 4-aminopyridine, respectively, were dissolved in water (5 cm^3) and heated at 373 K in closed teflon vessel for *c.a.* 1 day. Crystals of **1-a**, **2-a** and **3-a** were obtained after slow evaporation of the resulting solutions (pH = 5,46, 5.65, 5,62, respectively) combined with diffusion of 2-propanol.

Crystal structure determination
The crystallographic measurements for **1-a**, **2-a** and **3-a** were performed on a Kuma KM4-CCD (**1-a**, **3-a**) or Xcalibur PX (**2-a**) automated four-circle diffractometers with the graphite-monochromatized Mo-K_α radiation at 250(2) K (**1-a**, **2-a**) or 100(2) K (**3-a**). The X-ray data for **1-a** and **2-a** were collected at 250(2) K owing to poor diffraction pattern at 100 K. Data collection, cell refinement, and data reduction and analysis were carried out with CrysAlisCCD and CrysAlisRED, respectively.[16] Empirical absorption corrections were applied to the data with the use of CrysAlisRED. The structure of **2-a** was solved by direct methods using SHELXS-97,[17] and refined on F^2 by a full-matrix least-squares technique using SHELXL-97[17] with anisotropic thermal parameters for non-H atoms. The refinement for **1-a** and **3-a** was started by using the coordinates for non-H atoms of **2-a** (excepting water molecules). The non-H atoms in **1-a**–**3-a** were refined anisotropically, except for low-occupied positions of disordered H_2O.

The O atoms of two water molecules (O2*W* and O4*W*) in **1-a** and **2-a** are disordered over two sites (with s.o.f. = 0.73(3)/0.27(3) for O2*W* and 0.70(4)/0.30(4) for O4*W* in **1-a**, and 0.71(3)/0.29(3) and 0.78(4)/0.22(4) for **2-a**). The disordered O2*W* and O4*W* in both **1-a** and **2-a** were refined with the common H atoms positions (s.o.f. for H atoms = 1.0). In **3-a**, O2*W* and O3*W* were found to have one H atom disordered over two sites (refined with s.o.f. = 0.5). O4*W* in **3-a** is disordered into two positions (s.o.f. = 0.73(3) and 0.27(3)), each of them having different locations of both H atoms. Some of the bisphosphonate H atoms in **1-a** and **2-a** are disordered over two sites (denoted as H2, H3, H5, H6 in **1-a**, and H2, H3 in **2-a**) and were refined with s.o.f. = 0.5 each, at two different O atoms (O2/O3 or O5/O6). All H atoms were found in difference Fourier maps. In the final refinement cycles, all water H atoms were refined with O–H and H···H distances restrained to 0.84 and 1.38 Å, respectively, and with U_{iso}(H) = 1.5U_{eq}(O). All remaining H atoms were treated as riding atoms in geometrically optimized positions, with O–H = 0.83–0.84 Å, N–H = 0.87–0.88 Å and C–H = 0.94–1.00 Å, and with U_{iso}(H) = 1.5U_{eq}(O) or 1.2U_{eq}(N,C). The figures were made using DIAMOND program.[18]
A summary of the conditions for the data collection and the structures refinement parameters are given in Table 4.

Table 4. Crystal data and structure refinement details for **1-a**–**3-a**

	1-a	**2-a**	**3-a**
Formula	$C_{16}H_{29}ClN_6O_{10}P_2$	$C_{16}H_{29}BrN_6O_{10}P_2$	$C_{16}H_{29}IN_6O_{10}P_2$
Formula weight [g mol^{-1}]	562.84	607.30	654.29
Crystal system	triclinic	triclinic	triclinic
Space group	$P\bar{1}$	$P\bar{1}$	$P\bar{1}$
a [Å]	9.587(5)	9.576(3)	9.584(3)
b [Å]	11.128(5)	11.214(3)	11.473(4)
c [Å]	13.310(5)	13.381(4)	13.206(4)
α [°]	94.80(5)	94.08(3)	94.16(3)
β [°]	102.35(5)	102.44(3)	104.72(3)
γ [°]	113.39(5)	113.37(3)	113.95(3)
V [Å^3]	1250.4(10)	1268.3(6)	1257.9(7)
Z	2	2	2
D_{calc} [g cm^{-3}]	1.495	1.590	1.727
μ [mm^{-1}]	0.34	1.81	1.46
F(000)	588	624	660
Crystal colour and form	colourless columnlike plate	colourless columnlike block	colourless plate
Crystal size [mm]	0.28 × 0.04 × 0.02	0.20 × 0.13 × 0.05	0.33 × 0.10 × 0.07
Radiation type; λ [Å]	Mo-K_α; 0.71073	Mo-K_α; 0.71073	Mo-K_α; 0.71073
T [K]	250(2)	250(2)	100(2)
θ range [°]	3.02–30.00	4.20–30.00	2.66–30.00

Indexes ranges	$-10 \le h \le 12$	$-11 \le h \le 13$	$-8 \le h \le 13$
	$-14 \le k \le 14$	$-15 \le k \le 15$	$-15 \le k \le 16$
	$-18 \le l \le 17$	$-18 \le l \le 18$	$-17 \le l \le 18$
Measured reflections	13395	27648	15639
Independent reflections	6252 [R_{int} = 0.050]	7380 [R_{int} = 0.104]	6691 [R_{int} = 0.023]
Observed refl. ($I > 2\sigma(I)$)	2905	2968	5857
Absorption correction	empirical	empirical	empirical
T_{min}/T_{max}	0.990/1.000	0.770/1.000	0.834/1.000
Data/restraints/parameters	6252/16/354	7380/16/353	6691/19/359
$R1$; $wR2$ ($F_o^2 > 2\sigma(F_o^2)$)[a]	0.050, 0.056	0.045, 0.055	0.026, 0.062
$R1$; $wR2$ (all data)[a]	0.131, 0.061	0.153, 0.059	0.033, 0.065
GooF = S	1.03	1.01	1.04
$\Delta\rho_{max}/\Delta\rho_{min}$ [e Å^{-3}]	0.29/-0.31	0.52/-0.38	0.71/-0.41

[a] $R1 = \sum \| |F_o| - |F_c| \| / \sum |F_o|$; $wR2 = \sqrt{\sum [w(F_o^2 - F_c^2)^2] / \sum [w(F_o^2)^2]}$

NMR measurements

The NMR spectra were recorded on a Bruker DRX spectrometer operating at 121.50 MHz for ^{31}P and 300.13 MHz for ^{1}H at 300 K, unless otherwise noted, and are given in relation to 85% H_3PO_4 and $SiMe_4$, respectively. All downfield shifts are denoted as positive. Samples for NMR studies were prepared in deuterated water with a metal(II) concentration of 1 x 10^{-2} M and M(II)-to-ligand molar ratios of 1:1 and 1:2. The measurements were performed only for freshly prepared samples. The variable temperature ^{31}P NMR spectra of **3** were performed on the Bruker DRX 600 MHz spectrometer over a temperature range 298-228 K. The sample was prepared by mixing of 0.05 M water (D_2O) solution of pH 5.5 with methanol-d4 at 2:3 v/v ratio. No correction was made for temperatures indicated by the VT unit.

The pH was measured using a Radiometer pHM83 instrument equipped with a Metler Toledo INLAB 422 combined electrode and is given as meter readings without correction for pD.

Potentiometric measurements

The potentiometric titrations were performed in 3 cm^3 samples. The ligand concentration was 2 x 10^{-3} mol dm^{-3}. The metal-to-ligand ratios ranged from 1:1 to 1:3.5, three or four different ratios were applied for each system studied. The samples were titrated in the pH range 2.5-11. The potentiometric titrations were performed using an automatic titrator system Titrando 809 (Metrohm) with a Metrohm 6.0234.100 type combined glass electrode filled with 3 M KCl in water. The measurements were carried out in an argon atmosphere at 298 K at constant ionic strength (0.2 mol dm^{-3} KCl).

The protonation constants of the ligand and the concentration stability constants ($\log\beta_{pqr}$) of the metal complexes were calculated by means of a general computational program, SUPERQUAD[19]. The uncertainties (3SD values) of the stability constants are given in

parentheses in Table 3. The electrode system was calibrated daily in hydrogen ion concentration using HCl solution (0.02 mol dm^{-3} in KCl) against standard KOH solution (0.15 mol dm^{-3}). The water ionization constant (pK_w) determined was 13.74 ± 0.01. The calibration of the electrode was as pH = -log[H^+]. The stability constants of M^{2+}–OH systems were included in the calculations and were taken from the literature.[20] The charges of the complexes have been omitted in the text, Table and Figures. However, for clarity, it should be mentioned that the fully deprotonated form of ligand is L^{4-}.

ESI-MS measurements. ESI-MS experiments for the M(II)–**3** systems (M – Zn, Mg, Ca) were performed on a Bruker MicrOTOF-Q spectrometer (Bruker Daltonic, Bremen Germany) equipped with an Apollo II electrospray ionization source with an ion funnel. The spectra were acquired in both positive and negative ion mode.
The experiments were performed for the solutions with 1:1 and 1:2 metal-to-ligand molar ratios. Stock aqueous solutions of samples were prepared at concentrations corresponding to the NMR studies. The pH was set between *c.a.* 6.5–11 by an addition of the desired amount of KOH or NaOH (Ca(II) systems). Routinely the 50:50 (v/v) MeOH/H_2O samples were measured. However, the variations of the analyte composition down to 5% of MeOH did not change the species composition.
Samples were infused into the ESI source at a flow rate of 3 μl/min. Before each run, the instrument was calibrated externally with the Tunemix™ mixture (Bruker Daltonik, Germany) in quadratic regression mode. The instrumental parameters were as follows: the scan range *m/z* 200–2000, end plate offset -500 V, dry gas nitrogen (4 L/min), temperature 473 K, capilary voltage 4500 V, ion energy 5 eV. Data analysis was carried out with the use of Bruker Daltonics Data Analysis software *v. 3.4*.

Suplementary Data

CCDC 846051 (**1-a**), 846052 (**2-a**), 846053 (**3-a**) contain the supplementary crystallographic data for this paper. These data can be obtained free of charge via http://www.ccdc.cam.ac.uk/conts/retrieving.html, or from the Cambridge Crystallographic Data Centre, 12 Union Road, Cambridge CB2 1EZ, UK; fax: (+44) 1223-336-033; or e-mail: deposit@ccdc.cam.ac.uk.
Gometrical parameters and symmetry codes of proposed hydrogen bonds and close contacts for **1-a, 2-a** and **3-a** are given as supplementary material in Table S1.

Acknowledgements

We express our gratitude to Prof. Paweł Kafarski for supplying the samples of the studied aminobisphosphonates. Financial support from the Chemistry Department, Wrocław University

of Technology, Grant No S10064/Z0304 (E.M.J.) and from Faculty of Chemistry, University of Opole (B.K.) is gratefully acknowledged.

References

1. (a) Shane, E.; Burr, D.; Ebeling, P. R. et al. *J. Bone Mineral Res.* **2010**, *25*, 2267. (b) Russell, R. G. G.; Watts, N. B.; Ebetino, F. H.; Rogers, M. J. *Osteoporos Int.* **2008**, *19*, 733.
2. Oldfield, E. *Acc. Chem. Res.* **2010**, *43*, 1216. (b) Dunford, J. E.; Kwaasi, A. A.; Rogers, M.; Barnett, B. L.; Ebetino, F. H.; Russell, R. G. G.; Oppermann, U.; Kavanagh, K. L. *J. Med. Chem.* **2008**, *51*, 2187.
3. Suzuki, F.; Fujikawa, Y.; Yamamoto, S.; Mizutani, H.; Ohya, T.; Ikai, T.; Oguchi, T. *Ger. Offen*., 2.831, 578, 1979.
4. (a) Leon, A.; Liu, L.; Yang, Y.; Hudock, M. P.; Hall, P.; Yin, F.; Studer, D.; Puan, K.-J.; Morita, C. T.; Oldfield, E. *J. Med. Chem.* **2006**, *49*, 7331. (b) Ghosh, S.; Chan, J. W.; Lea, Ch. R.; Meints, G. A.; Lewis, J. C.; Tovian, Z. S.; Flessner, R. M.; Loftus, T. C.; Bruchhaus, I.; Kendrick, H.; Croft, S. L.; Kemp, R. G.; Kobayashi, S.; Nozaki, T.; Oldfield, E. *J. Med. Chem.* **2004**, *47*, 175.
5. (a) Sanders, J. M.; Gomez, A. O.; Mao, J.; Meints, G. A.; Van Brusel, E. M.; Burzyńska A.; Kafarski, P.; Gonzalez-Pacanowska, D.; Oldfield, E. *J. Med. Chem.* **2003**, *46*, 5171. (b) Sanders, J. M.; Song, J.; Chan, J. M. W.; Zhang, Y.; Jennings, S.; Kosztowski, T.; Odeh, S.; Flessner, R.; Schwerdtfenger, Ch.; Kotsikoru, E.; Meints, G. A.; Gómez, A. O.; González-Pacanowska, D.; Raker, A. M.; Wang, H.; van Beck, E. R.; Papapoulous, S.; Morita, C. T.; Oldfield, E. *J. Med. Chem.* **2005**, *48*, 2957.
6. (a) Matczak-Jon, E.; Sawka-Dobrowolska, W.; Kafarski, P.; Videnova-Adrabińska, V. *New J. Chem*. **2001**, *25*, 1447. (b) Szabo, C. M.; Martin, M. B.; Oldfield, E. *J. Med. Chem.* **2002**, *45*, 2894.
7. Matczak-Jon, E.; Ślepokura, K.; Zierkiewicz, W.; Kafarski, P.; Dąbrowska, E. *J. Mol. Struct*. **2010**, *980*, 182.
8. (a) Matczak-Jon, E.; Ślepokura, K.; Kafarski, P. *J. Mol. Struct*. **2006**, *782*, 81. (b) Matczak-Jon, E. *Pol. J. Chem*. **2005**, *79*, 445.
9. (a) Matczak-Jon, E.; Ślepokura, K.; Kafarski, P. *Acta Cryst. C* **2006**, *62*, o132. (b) Matczak-Jon, E.; Ślepokura, K.; Kafarski, P.; Skrzyńska I. *Acta Cryst. C* **2009**, *65*, o261.
10. Matczak-Jon, E.; Kowalik-Jankowska, T.; Ślepokura, K.; Kafarski, P.; Rajewska, A. *Dalton Trans*. **2010**, *39*, 1207.
11. Di Marco V, B.; Bombi, G. G. *Mass Spectrom. Rev*. **2006**, *25*, 347.
12. Colton, R.; D'Agostino, A.; Traeger, J. C. *Mass Spectrom. Rev.* **1995**, *14*, 79.
13. Matczak-Jon, E.; Kurzak, B.; Sawka-Dobrowolska, W. *Polyhedron*, **2012**, *31*,17.
14. Sołoducho, J.; Gancarz, R.; Wieczorek, P.; Korf, J.; Hafner, J.; Lejczak, B.; Kafarski, P. Patent PL 172268 B1, 1997.

15. Gran, G. *Acta Chem. Scand*. **1950**, *4*, 559.
16. CrysAlis RED, ver. 1.171 Oxford Diffraction Poland, 1995-2003.
17. Sheldrick, G. M. SHELXL-97 and SHELXS-97, University of Göttingen, Germany, 1997.
18. Brandenburg, K. DIAMOND, ver. 3.0, Crystal Impact GbR, Bonn, Germany, 2005.
19. Gans, P.; Sabatini, A.; Vacca, A. *J. Chem. Soc. Dalton Trans*. 1**985**, 1195.
20. Baes, C. F.; Mesmer, R. E. *The Hydrolysis of Cations*, Wiley-Interscience, New York 1976.

